Two-Photon Absorption in Quadrupolar π-Conjugated Molecules: Influence of the Nature of the Conjugated Bridge and the Donor–Acceptor Separation

Egbert Zojer,*[a, b, d] David Beljonne,[c] Peter Pacher,[a] and Jean-Luc Brédas*[a, d]

Abstract: Quadrupolar-type substitution of π-conjugated chromophores with donor and acceptor groups has been shown to increase their two-photon absorption (TPA) response by up to two orders of magnitude. Here, we apply highly correlated quantum-chemical calculations to evaluate the impact of the nature of conjugated bridge and the charge-transfer distance on that enhancement. We compare chromophores with phenylenevinylene-, thienylenevinylene-, polyene-, and indenofluorene-type backbones substituted by dimethylamino and cyano groups. In all compounds, we find a strongly TPA-active A_g state (either $2A_g$ or $3A_g$) in the low-energy region, as well as a higher lying TPA-active state (mA_g) at close to twice the energy of the lowest lying one-photon allowed state; the smaller energy detuning in the mA_g states results in very large TPA cross sections δ. We also investigate the influence of the degree of ground-state polarization on TPA. Independent of the nature of the backbone and the donor–acceptor separation, δ displays the same qualitative evolution with a maximum before the cyanine-like limit; the highest TPA cross sections are calculated for distirylbenzene- and polyene-based systems.

Keywords: computer chemistry · electron correlation · nonlinear optics · structure–property relationships · two-photon absorption

Introduction

Two-photon absorption (TPA) in organic molecules is receiving considerable attention owing to a number of promising applications. These include optical limiting,[1] 3D microfabrication and optical data storage,[2] 3D fluorescence microscopy,[3] and biological caging.[4] These applications exploit the increased spatial resolution and improved penetration depth typical of nonlinear absorption processes.

Chromophores with large TPA cross sections (δ) are highly desirable for the exploitation of TPA processes at moderate laser intensities. In order to develop strategies for the design of compounds that combine high TPA cross sections with other useful optical or chemical properties (such as high fluorescence quantum yields or low excited-state oxidation potentials), a detailed understanding of the relationship between the chemical structure of a molecule and its TPA characteristics is required. It has been shown that donor and/or acceptor substitution of conjugated molecules results in a marked increase of δ.[5] Dipolar,[6–8] quadrupolar,[5,6,9,10] octupolar,[11,12] as well as dendrimeric[13] systems have been studied in great detail. Drobizhev et al. also found large δ values for symmetrically acceptor-substituted porphyrins.[14] Our recent work on stilbene derivatives revealed that the increased TPA cross section associated with donor and acceptor substitution and its dependence on the donor–acceptor strength result from electron correlation effects.[15]

Here, we investigate the influence of the conjugated path on the TPA response in quadrupolar chromophores by varying the chemical nature of the π-electron system, the effective conjugation length, and the donor–acceptor separation (i.e., the charge-transfer distance, both parallel and perpendicular to the long molecular axis). For all molecular backbones studied here, the evolution of δ is monitored as a function of the degree of ground-state polarization. A

[a] Prof. E. Zojer, P. Pacher, Prof. J.-L. Brédas
Department of Chemistry, The University of Arizona
Tucson, Arizona 85721-0041 (USA)
Fax: (+1) 404-894-7452

[b] Prof. E. Zojer
Institut für Festkörperphysik
Technische Universität Graz
Petersgasse 16, 8010 Graz (Austria)

[c] Dr. D. Beljonne
Service de Chimie des Matériaux Nouveaux
Centre de Recherche en Electronique et Photonique Moléculaires
Université de Mons-Hainaut, 7000 Mons (Belgium)

[d] Prof. E. Zojer, Prof. J.-L. Brédas
School of Chemistry and Biochemistry
Georgia Institute of Technology
Atlanta, Georgia 30332-0400 (USA)
Fax: (+1) 404-894-7452
E-mail: egbert.zojer@chemistry.gatech.edu
jean-luc.bredas@chemistry.gatech.edu

DOI: 10.1002/chem.200305650

simple three-state model is applied to interpret the various contributions to TPA.

Theoretical approach

The model systems: The chemical structures of the π-conjugated molecules considered here are shown in Figure 1.

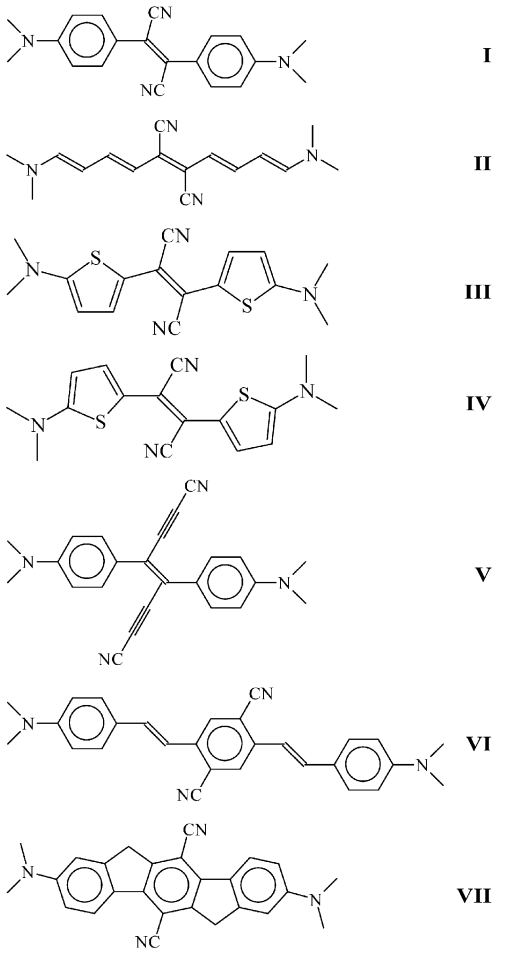

Figure 1. Chemical structures of the donor/acceptor-substituted molecules investigated in the present study.

They are bis(dimethylamino)bis(cyano)-substituted chromophores with phenylenevinylene (stilbene and distirylbenzene), polyene, thienylenevinylene, and indenofluorene backbones (note that **III** and **IV** correspond to two conformers of the same molecule). The evolution of the resonant nonlinear optical properties was studied with the approach that we previously applied with success to determine hyperpolarizabilities[16–18] and TPA cross sections[8,15] in donor/acceptor-substituted chromophores. Unless otherwise stated, the backbones of these model systems are kept planar; however, the consequences of allowing for a twist between the phenylene/thienylene rings and the vinylene unit(s) will be briefly discussed below (they have also been studied both experimentally and theoretically in ref. [19] for phenylenevinylene derivatives).

To modulate the degree of ground-state polarization in such quadrupolar molecules, a set of point charges is placed above and below the nitrogen atoms of the dimethylamino and cyano substituents along the normal to the molecular plane, as shown in Figure 2 for molecule **VI**.[15,20] The point charges create a quadrupole-like electric field that promotes charge transfer from the donor to the acceptor groups, as discussed in detail in reference [15]. Decreasing the distance

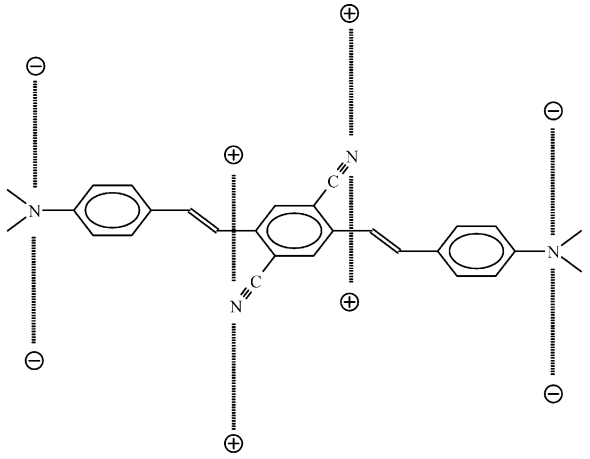

Figure 2. Donor/acceptor-substituted distirylbenzene with point charges used to create an additional quadrupolar field in the plane of the molecule.

(d) between the point charges and the nitrogen atoms allows a systematic tuning of the degree of ground-state polarization. Experimentally, the ground-state polarization can be modulated by changing the actual strength of the donor/acceptor substituents and/or the polarity of the medium.[21]

Describing the TPA response: We calculated the TPA response by means of the two-photon absorption tensor $S_{e'}$. For degenerate TPA (i.e., the simultaneous absorption of two photons from a single monochromatic laser beam) into a particular two-photon excited state $|e'\rangle$, $S_{e'}$ is given by Equation (1):[22,23]

$$S^{i,j}_{e'} = \sum\nolimits_{e} \left(\frac{M^{i}_{ge} M^{j}_{ee'}}{E_{ge} - E_{ge'}/2} + \frac{M^{j}_{ge} M^{i}_{ee'}}{E_{ge} - E_{ge'}/2} \right) \quad (1)$$

In Equation (1) $E_{ge'}/2$ corresponds to the energy of the incident photons. M_{ge} and $M_{ee'}$ are the transition dipoles between the ground state $|g\rangle$and an intermediate one-photon state $|e\rangle$ and between $|e\rangle$ and $|e'\rangle$, respectively. E_{ge} and $E_{ge'}$ are the corresponding transition energies and the indices i and j represent the Cartesian coordinates. In our studies, 300 intermediate states are considered to ensure fully converged results. In an isotropic medium and for a linearly polarized excitation source, $S_{e'}$ is related to the corresponding TPA cross section by Equations (2):[22,24]

$$\bar{\delta}^{e'}_{TEN} \propto \frac{1}{15} \sum\nolimits_{i,j} \left(S^{*ii}_{e'},\ S^{*jj}_{e'} + 2\, S^{*ij}_{e'} S^{*ij}_{e'} \right) \quad (2)$$

Combining the cross sections from Equation (2) for all TPA-active states $|e'\rangle$ with normalized line-shape functions then yields the overall TPA response.

To ease the analysis of the calculated trends, it is helpful to derive an approximate expression for Equations (1) and (2): for centrosymmetric molecules and provided that a single excited state $|e\rangle$dominates the low-energy region of the linear optical spectrum, one finds for the TPA resonance into $|e'\rangle$ [Eq. (3)]:[5,25]

$$\delta^{e\prime}_{\text{approx}} = \frac{(E_{ge\prime}/2)^2}{5\,c^2\varepsilon_0\hbar}\,\frac{M^2_{ge}M^2_{ee'}}{(E_{ge}-E_{ge'}/2)^2\Gamma} \tag{3}$$

In the course of our discussions, the evolution of the TPA cross section as a function of the degree of ground-state polarization will be analyzed on the basis of the quantities dominating Equation (3). These are: 1) the detuning factor between the one- and two-photon states, $(E_{ge}-E_{ge}/2)$; 2) the transition dipole between the ground state and the one-photon state, M_{ge}; and 3) the transition dipole between $|e>$ and $|e'>$, $M_{ee'}$ (by means of the effective value calculated according to ref. [10]).

Transition densities: To analyze the characteristics of the transition dipoles $\overrightarrow{M_{AB}}$ that appear in Equation (3), it is useful to recall that they are defined as in Equation (4):

$$\begin{aligned}\overrightarrow{M_{AB}} &= e\int \rho_{A\to B}(\vec{r})\,\vec{r}\,d^3r\\ \rho_{A\to B}(\vec{r}) &= \Psi^*_A\Psi_B(\vec{r})\\ &= N\int \Psi^*_A(\vec{r},\vec{r_2},\ldots\vec{r_N})\Psi_B(\vec{r},\vec{r_2},\ldots\vec{r_N})d\vec{r_2},\ldots\vec{r_N}\end{aligned} \tag{4}$$

In Equation (4) $\rho_{A\to B}(\vec{r})$ is the transition density between states A and B at point $\vec{r}$ in space. The choice of the origin of coordinates does not affect the results and can thus be conveniently taken to coincide with the molecular center of inversion. For the semiempirical methods employed here, we will replace the full expression for $\rho_{A\to B}(\vec{r})$ by the transition densities that are associated with the individual atoms employing the ZDO approximation.

From Equation (4), we see that in order to maximize the transition dipole between two states, it is important that: 1) the overlap between the wavefunctions Ψ_A and Ψ_B be maximized, 2) transition densities far from the center of inversion be large, and 3) atomic transition densities on the same side of the molecule have the same sign. (Note that for optically allowed transitions, the signs on opposite sides of the center of inversion have to be different to satisfy parity selection rules.)

Results and Discussion

In order to describe more completely the microscopic origin for the TPA response in quadrupolar-type chromophores, we have investigated the conjugated backbones shown in Figure 1. Starting from stilbene (**I**), we have considered: 1) more easily polarizable conjugated backbones: polyene (**II**) and thienylenevinylene (**III** and **IV**), 2) more extended conjugated paths: one including triple bonds leading to a larger separation between the stilbene and the acceptor groups (**V**), the other corresponding to distirylbenzene (**VI**) with an increased conjugation length, and 3) indenofluorene (**VII**).

Dependence of the TPA cross section on the nature of the conjugated backbone: The calculated TPA cross sections as well as the terms entering the 3-state expression for δ [Eq. (3)] are given in Table 1 for the molecules of Figure 1 in their planar conformation. In all molecules, there is a strongly two-photon allowed state in the low-energy region, $2A_g$ or $3A_g$ (the very small δ values for $2A_g$ in **II**, **III**, and

Table 1. TPA cross sections (with δ_{TEN} referring to the converged result including 300 excited states and δ_{approx} to the three-state approximation), transition energies, and transition dipoles for the lowest lying two-photon allowed states (i.e., states with gerade symmetry). Also the energies and transition matrix elements for the lowest one-photon states are given. (1 GM corresponds to 10^{-50} cm^4 s photon^{-1}). The angles between the arylene and vinylene segments in the non-planar conformations are: 47° (**I**), 43° (**III**), 50° (**V**), 26°, 12° (**VI**).

	One-photon absorption			Two-photon absorption					
		E_{ge}[Ev]	M_{ge}[debye]		$E_{ge'}$[eV]	$(E_{ge'}/2)/(E_{ge}-E_{ge}/2)$	$M_{ee'}$[debye]	δ_{TEN}[GM]	δ_{approx}[GM]
planar									
I	S_1–$1B_u$	3.22	8.51	S_2–$2A_g$	3.79	1.43	12.85	446	512
II	S_2–$1B_u$	3.08	10.52	S_1–$2A_g$	2.99	0.94	3.60	28	26
				S_4–$3A_g$	4.00	1.86	13.96	1500	1560
III	S_2–$1B_u$	2.65	9.28	S_1–$2A_g$	2.61	0.97	1.93	9	6
				S_4–$3A_g$	3.59	2.09	11.91	1092	1119
IV	S_2–$1B_u$	2.70	8.82	S_1–$2A_g$	2.58	0.91	1.70	6	4
				S_4–$3A_g$	3.65	2.08	10.49	772	780
V	S_1–$1B_u$	3.14	8.06	S_2–$2A_g$	3.75	1.48	11.07	345	365
VI	S_1–$1B_u$	3.34	11.27	S_2–$2A_g$	3.87	1.37	17.22	1151	1486
VII	S_1–$1B_u$	3.41	7.53	S_3–$2A_g$	4.12	1.53	12.40	499	429
non-planar									
I	S_1–1u	3.70	6.24	S_2–2g	4.02	1.19	13.83	166	222
III	S_1–1u	3.09	6.79	S_2–2g	3.22	1.09	6.61	45	50
				S_3–3g	3.84	1.65	8.99	193	213
V	S_1–1u	3.54	6.34	S_2–2g	3.68	1.08	8.44	57	70
VI	S_1–1u	3.55	10.05	S_2–2g	4.07	1.35	16.98	836	1104

IV will be discussed in detail below). The trends obtained for δ_{approx} (i.e., when applying the 3-state model) closely follow those of the converged TPA cross sections calculated with the complete two-photon tensor.[26] This allows an analysis of the factors that enhance TPA based on the relative energies of the $1B_u$ and $2A_g/3A_g$ states and the corresponding transition dipole moments.

Taking **I** as the system of reference (and considering TPA into the larger of 2Ag and 3Ag), we observe that switching to less aromatic rings as in **III**/**IV** allows for an increase in δ by a factor of 2–2.5, depending on the conformation. On the other hand, switching to a phenylene (indenofluorene) backbone with the same number of carbons along the conjugated path as in **VII** has little influence. Elongating the backbone in **VI** produces an increase with a factor of 2.5. The largest increase (factor >3) is calculated when considering a polyene backbone, which is known to be highly polarizable. These results are in agreement with what is known from organic nonlinear optics (see, for instance, ref. [17]).

As indicated above, the largest cross sections are obtained for molecules **II** and **VI**. In the case of **II**, this is caused by a combination of (rather) large values for the transition dipole moment between the ground state and the one-photon state (M_{ge}), the energy-related term $[(E_{ee'}/2)/(E_{ge}-E_{ee'}/2)]$ (resulting from a relatively small detuning between the $1B_u$ state and half the energy of the $3A_g$ state), and the transition dipole moment between the one- and two-photon states ($M_{ee'}$). At this stage, it is worth recalling that the increased $M_{ee'}$ coupling has been originally identified as the main reason for the strongly enhanced TPA cross sections in donor/acceptor substituted systems.[5] While in **II** all terms entering the 3-state expression for δ are large, there is a significant detuning in **VI** (large difference between E_{ge} and $E_{ee'}/2$), which is nearly compensated by the exceptionally large value of $M_{ee'}$.

To evaluate the impact of intramolecular torsion, we have also included the δ values calculated for fully relaxed, nonplanar conformations of molecules **I**, **III**, **V**, and **VI** with C_i symmetry.[27] Twist angles vary from 50° between the central vinylene unit and the phenylenes in **V**, to 26° between the central ring and the vinylenes and 12° between the vinylenes and the outer rings in **VI** (in **I** and **III**, the torsion angles are in the order of 47° and 43°, respectively). As expected, departure from planarity leads to a decrease in the TPA cross sections. This effect is strongest for molecule **III** and weakest for molecule **VI**. The reduced conjugation leads to a blue-shift of the $1B_u$ state relative to the excited A_g states (resulting in an increased detuning) and a reduced coupling between the ground state and the lowest one-photon state (i.e., a smaller transition dipole moment M_{ge}). In all molecules except **I**, one also observes a reduction of $M_{ee'}$. In **III**, there is in fact a redistribution of oscillator strength between the two lowest lying excited states of *g* symmetry in the twisted conformation.

To the best of our knowledge, molecule **VI** (with dibutylamino instead of dimethylamino substituents) is the only molecule studied here for which experimental data have been reported.[19] The calculated transition matrix elements in Table 1[28] ($M_{ge}=10.05$ D and $M_{ee'}=16.98$ D) are in excellent agreement with the measured values ($M_{ge}=10.0$ D and $M_{ee'}=15.1$ D). The calculated transition energies overestimate the experimental results (maxima at 2.53 eV for E_{ge} and 1.49 eV for the energy of the TPA resonance). This results in too large a detuning and, therefore, in a somewhat underestimated TPA cross section (experimental value of 1750 GM vs a calculated value of 1104 GM). This difference partly results from an overcorrelation (overstabilization) of the ground state in the MRDCI approach.[5]

In the following, we will restrict the discussion to planar structures, since our main goal is to establish general relationships between the chemical nature of quadrupolar-type molecules and their TPA cross sections. However, it must be borne in mind that it is important to prevent large ring twists, for example, by planarizing the structure and avoiding unfavorable substitution patterns (such as those where cyano groups are attached directly or through linkers to the vinylene segments, as in molecules **I**, **III**, and **V**).

Evolution of the transition densities: To obtain a better understanding of the dependence of the transition dipoles on the chemical structure of the backbones, it is useful to analyze the corresponding transition densities. Those describing the couplings between the ground state and the lowest one-photon state and the one-photon and lowest two-photon active states are shown in Figure 3 for molecules **I**, **V**, and **VI**, and in Figure 4 for molecule **II**.

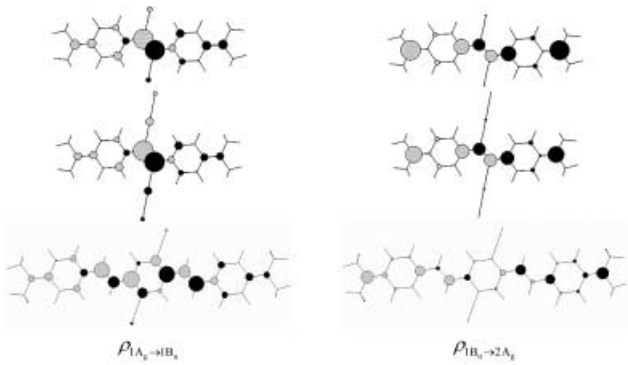

Figure 3. ZDO transition densities for the $1A_g$ to $1B_u$ and the $1B_u$ to $2A_g$ excitations in molecules **I**, **VI**, and **VII**. The diameter of the circles is proportional to the transition density associated with each atom and the shading represents the sign of the transition density.

As mentioned above, it is desirable to have large transition densities present at the extremities of the molecule; in which case, the $\vec{r}$ factor in Equation (4) is largest and the resulting transition dipoles are high. For the $1B_u \rightarrow 2A_g$ transitions (for **I**, **V**, **VI**, and **VII**) or $1B_u \rightarrow 3A_g$ transitions (for **II**, **III**, **IV**), this is achieved primarily through the addition of the terminal donor substituents. As shown in the bottom part of Figure 3, the transition densities have large contributions on the nitrogen atoms of the dimethylamino groups. This rationalizes the very large value of $M_{ee'}$ in molecule **VI**, in which the distance between the atoms on the two ends of the molecule bearing the large transition densities is larger

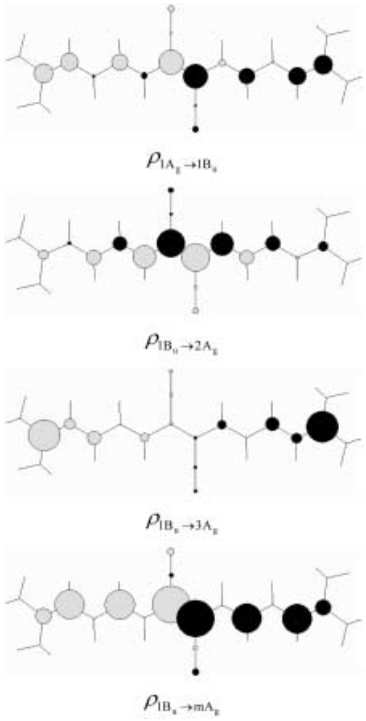

Figure 4. ZDO transition densities for the excitations most relevant for the TPA absorption properties of molecule **II**. The diameter of the circles is proportional to the transition density associated with each atom and the shading represents the sign of the transition density.

than in the other systems. In general, the conjugation-length dependence of the TPA cross section can be expected to arise from a compromise between the increased charge-transfer distance for longer molecules, which increases the TPA response, and the decoupling between the donor and acceptor groups beyond a certain size of the molecule.[29]

In contrast to the significant increase of $M_{ee'}$ for larger distances between the donor groups along the long axis of the molecules, increasing the distance between the acceptor groups and the conjugated backbone in a direction *perpendicular to the long molecular axis* (as in **V**) does not result in an increase of δ compared to **I**. This can be explained by the fact that the transition densities in **V**, corresponding to M_{ge} and $M_{ee'}$, do not extend over the acceptor units and in fact hardly change compared to **I**, as shown in Figure 3. To ensure that this is not primarily the consequence of a possible weakening of the acceptor strengths of the CN groups caused by the triple bonds in **V**, we also investigated a variation of molecule **VI** in which we introduced vinylene units between the central ring and the CN groups; here too, no significant increase of δ was calculated.

Another important characteristic of transition densities are their relative signs (phases) on adjacent atoms. The impact on the transition dipoles can be most clearly illustrated for molecule **II** (Figure 4). For the $1A_g \rightarrow 1B_u$ transition, all significant transition densities on one side of the molecule are positive, while they are negative on the other side. As a result, M_{ge} in **II** is nearly as large as in **VI**, although **VI** is 5.3 Å longer; in **VI**, the transition densities for $1A_g \rightarrow 1B_u$ on each half of the molecule partly cancel. Cancellation effects resulting from a sign change of the transition densities on adjacent atoms are even more significant for the $1B_u \rightarrow 2A_g$ transition in **II** (Figure 4). They result in a very low cross section of only 28 GM for TPA into $2A_g$ in molecule **II**; in fact, $\rho_{1Bu \rightarrow 2Ag}$ is strongly reminiscent of the corresponding transition density distribution in unsubstituted polyenes,[30] which lack the enhancement effects owing to the donor/acceptor substitution. In contrast, the $1B_u \rightarrow 3A_g$ transition density in **II** is strongly confined around the nitrogen atoms in the dimethylamino groups and there are no cancellation effects; this results in the very large cross section of 1500 GM for TPA excitation into $3A_g$. There are also no cancellation effects for the coupling between the $1B_u$ state and the so-called mA_g states, although the dimethylamino groups play a less important role there (Figure 4). This implies that the mA_g state should also have attractive TPA properties. At this point, it is interesting to mention that the $1B_u \rightarrow mA_g$ transition density in **II** is strongly reminiscent of what Heflin et al. described in the case of unsubstituted octatetraene for the $1B_u \rightarrow 6A_g$ transition;[30] this confirms that TPA into higher lying states should be very efficient in unsubstituted molecules as well.[30,31] We will turn to a discussion of TPA into these higher lying states in the next section.

At this stage, it is useful to classify the series of investigated molecules into two groups, depending on whether TPA into low-lying excited states occurs dominantly into the $2A_g$ or $3A_g$ state: group 1 then contains **I**, **V**, **VI**, and **VII**, while group 2 consists of **II**, **III**, and **IV**. Interestingly, group 2 molecules have their $2A_g$ state located below the $1B_u$ state. On the basis of extended Hubbard calculations on polyenes, Guo et al.[32] have shown that TPA into A_g states lying below $1B_u$ should be weak (the $2A_g$ state can be regarded as a pair of triplet excitations coupled to form a singlet, with weak coupling to the dominant one-photon $1B_u$ state), which is consistent with the small δ values for the $2A_g$ state that we calculate for all group 2 molecules. The existence of low-lying states with A_g symmetry in unsubstituted molecules is usually attributed to strong correlation effects (and a dominant covalent character).[30,31,33] For the donor/acceptor-substituted molecules, we also find that the $2A_g$ state is described by the mixing of several singly and doubly excited determinants with similar weights (vide infra), which is the signature of strong correlation effects.

We note that Soos and co-workers[31,34] have made a similar classification for centrosymmetric conjugated chains, depending on whether $2A_g$ or $1B_u$ is the lowest lying excited state (in the latter case, the system can be strongly fluorescent; in the former case, fluorescence is quenched). These authors have attributed the relative locations of $2A_g$ and $1B_u$ to differences in the effective alternation of the transfer integrals for various conjugated backbones[31] and site energy differences as a consequence of nonconjugated heteroatoms.[34]

TPA into higher lying excited states: In all molecules, we find a higher lying A_g state (denoted as mA_g), which displays a large dipole coupling to $1B_u$ and a high TPA cross section. Large TPA cross sections for higher lying states

with A_g symmetry have already been predicted for unsubstituted molecules.[30,31] The excited-state energies, transition dipoles, and TPA cross sections into mA_g states are summarized in Table 2. The transition dipoles that couple those states to the one-photon state ($M_{ee''}$) are comparable to

Table 2. TPA cross sections (with δ_{TEN} referring to the converged result including 300 excited states and δ_{approx} to the three-state approximation), transition energies, and transition dipoles for two-photon absorption to the mA_g state. (1 GM corresponds to 10^{-50} cm^{4}s/photon).

	$E_{ee''}$ [eV]	$(E_{ee''}/2)/(E_{ge}-E_{ee''}/2)$	$M_{ee''}$ [debye]	δ_{TEN} [10^3 GM]	δ_{approx} [10^3 GM]
planar					
I	4.80	2.92	8.79	0.72	0.75
II	5.10	4.81	14.75	12.09	11.67
III	4.75	8.65	12.58	21.30[a]	21.39
IV	4.79	7.76	12.84	16.40[a]	16.20
V	4.80	3.24	6.58	0.60	0.62
VI	5.64	5.41	12.52	12.48	12.20
VII	6.08	8.37	7.25	5.89[b]	4.37
nonplanar					
III	5.09	4.69	8.12	1.39	1.41
V	4.54	1.78	5.52	0.08	0.08
VI	5.89	4.90	9.91	5.26[b]	4.99

[a] Overlap with negative contributions lead to reduced δ values when applying the SOS approach (vide infra). [b] Several TPA-active states overlap in that energy range. Thus, the total cross section at a certain energy is larger than that predicted by calculations for TPA into a particular state $|e'\rangle$.

those found for the strongly allowed lower lying A_g states ($2A_g$ for group 1 and $3A_g$ for group 2 molecules). Since the transition energies to the mA_g states are getting close to twice those of the one-photon states, the detuning is strongly reduced [corresponding to a strong increase in the $(E_{ge'}/2)/(E_{ge}-E_{ge'}/2)$ term from Eq. (3)]. This results in an increase of the TPA cross section by about *one order of magnitude*. Admittedly, the absolute values of δ given in Table 2 have to be handled with care, as minor changes in the mA_g energy can result in very large changes in the detuning factor and, consequently, significant changes in the TPA cross sections. However, the important message is that in all molecules, except for the nonplanar conformation of molecule **I**, the $M_{ee''}$ transition dipoles into the mA_g states are comparable to those into the $2A_g/3A_g$ states; since the detuning factor related to mA_g is significantly reduced, a strongly increased TPA response is predicted.

Large δ values at relatively high energies are potentially interesting, for example, for improved resolution in 3D microfabrication at shorter wavelengths and in broadband optical-limiting applications. However, the problem one is facing when the detuning factor becomes very small (i.e., when approaching the double-resonance situation suggested, for example, in ref. [35]) is the increased overlap with linear absorption. Therefore, the extent to which the mA_g states can be beneficial for "pure" TPA applications (i.e., 3D microfabrication, imaging, etc.) mainly depends on the linear absorption linewidth. Here, bridged compounds can prove useful as they prevent the coupling of torsional vibrations to the electronic excitations and provide a more rigid backbone, two factors which usually contribute to sharp low-energy edges of the linear absorption features. As far as broadband optical limiters are concerned, overlap with weak linear absorption will be far less problematic and strong TPA concurrent with excited-state absorption can produce efficient broadband-limiting materials.

A close inspection of the electronic nature of mA_g reveals that it is closely related to $2A_g$ in group 1 molecules, and to $2A_g$ and $3A_g$ in the group 2 systems. The configuration interaction (CI) description of these states is dominated by the same configurations (Slater determinants). For the group 2 molecules, these are: 1) a determinant in which an electron has been promoted from the HOMO−1 to the LUMO, $|H-1\rightarrow L\rangle$; 2) a determinant with one electron promoted from the HOMO to the LUMO+1, $|H\rightarrow L+1\rangle$; and 3) a doubly excited determinant with two electrons promoted from the HOMO to the LUMO, $|H,H\rightarrow L,L\rangle$. The mixing of these three determinants gives rise to three excited states of A_g symmetry. As an example, the CI descriptions for **II** (in its planar conformation) are given in Scheme 1. A similar set of three states is found for the other group 2 molecules (**III** and **IV**).

$$0.52|H,H\rightarrow L,L\rangle + 0.44|H-1\rightarrow L\rangle - 0.36|H\rightarrow L+1\rangle + \ldots \quad (2A_g)$$

$$0.77|H-1\rightarrow L\rangle - 0.40|H\rightarrow L+1\rangle + \ldots \quad (3A_g)$$

$$0.56|H,H\rightarrow L,L\rangle + 0.55|H\rightarrow L+1\rangle + \ldots \quad (mA_g)$$

Scheme 1.

In the case of the group 1 molecules, only two determinants (namely, $|H-1\rightarrow L\rangle$ and $|H,H\rightarrow L,L\rangle$) dominate the CI descriptions of the lowest two TPA active states,[15] which in turn results in only two related TPA active states (namely, $2A_g$ and mA_g). The mixing among these configurations is of crucial importance for the oscillator strength redistribution effects discussed in the next section.

Tuning the degree of ground-state polarization: To study the evolution of δ with ground-state polarization, we have increased the charge transfer from the donor to the acceptor groups by applying a quadrupolar-type electric field as described in the Computational Methods section.[15] The evolution of δ_{TEN} as a function of the maximum field that these charges create along the long molecular axis[36] is shown in Figure 5. Here, we focus on the lowest lying strongly TPA-active state ($2A_g$ for group 1 and $3A_g$ for group 2 molecules). The value of the maximum electric field serves as a measure for the degree of induced ground-state polarization. Importantly, all molecules (apart from **VI**, as will be discussed below) show the same behavior: with increasing ground-state polarization, the TPA cross section strongly increases, reaches a maximum, and then collapses. Considering the broad variety of molecules studied here, this points to a common behavior for quadrupolar molecules, independ-

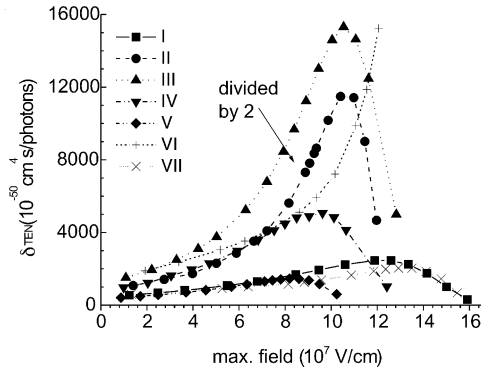

Figure 5. INDO/MRDCI calculated evolution of the converged TPA cross section into $2A_g/3A_g$ as a function of the strength of the donor and acceptor groups expressed as the maximum electric field along the molecular axis induced by the point charges. δ_{TEN} is derived from the TPA tensor as described in methodology section. The values of molecule **II** are divided by a factor of two to facilitate comparison.

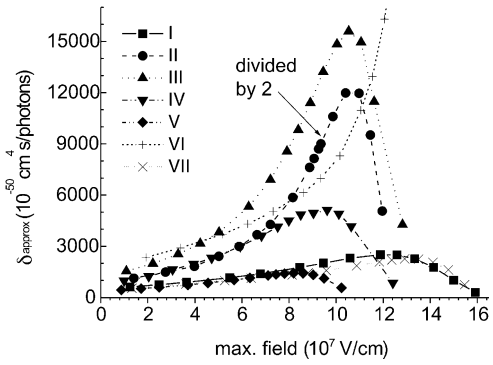

Figure 6. Evolution of the approximate TPA cross section δ_{approx}, derived from the three-state model, as a function of the maximum electric field along the long molecular axis induced by the point charges. The values for molecule **II** are divided by a factor of 2 to facilitate comparison.

ent of the actual nature of the conjugated backbone and of the charge-transfer distance. A qualitative deviation from this behavior appears to occur for molecule **VI**; however, the following discussion will show that the reasons for the sharp decrease in δ_{TEN} at large ground-state polarizations in all other molecules are also found in **VI**. The peculiar behavior observed in **VI** stems from a close to double resonance situation, which leads to a divergence in the transition-energy related part of the S tensor (but renders the molecule unsuitable for practical applications). Therefore, δ_{TEN} values for fields beyond $12\times10^7\,V\,cm^{-1}$ are not shown for **VI**.

To relate the evolution of δ to (a small number of) microscopic parameters, such as transition energies and transition dipoles, we have also investigated the evolution of δ_{approx} derived from the 3-state model given in Equation (3). The results are shown in Figure 6. They fully reproduce the trends obtained for the converged δ values. Thus, in the following, we will discuss the evolution of δ as a function of the ground-state polarization on the basis of the trends calculated for the transition dipoles between the ground state and one-photon states (M_{ge}) and between the one- and two-photon states ($M_{ee'}$), as well as for the corresponding transition energies (E_{ge} and $E_{ge'}$).

We start with an analysis of the transition energies: the ground-state polarization dependence of the energies for one-photon absorption (E_{ge}, corresponding to a transition to $1B_u$) and two-photon absorption ($E_{ge'}/2$, corresponding to a transition to $2A_g$ for group 1 molecules or to $3A_g$ for group 2 molecules, respectively) is shown in Figure 7, together with the energy-related term appearing in Equation (3), $[(E_{ge}/2)^2/(E_{ge}-E_{ge'}/2)^2]$. As expected, both E_{ge} and $E_{ee'}$ decrease with increasing ground-state polarization. It is interesting to note that the increased polarization quickly changes the order of the lowest lying excited states in the group 2 molecules: the $1B_u$ state comes to lie below $2A_g$ al-

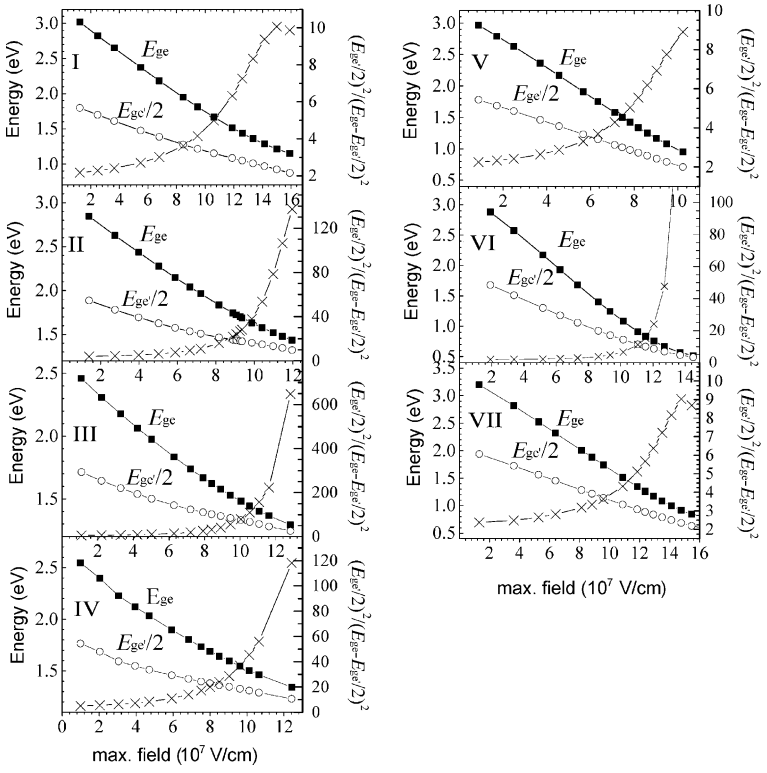

Figure 7. Evolution of the transition energies to the one-photon-allowed excited state (E_{ge}, ■) and half of the transition energies to the lowest strongly two-photon-allowed excited state ($E_{ge'}/2$, ○) as a function of the maximum electric field along the molecular axis induced by the point charges. The ×'s describe the evolution of the energy term entering the three level model [Eq. (3)].

ready for fields in the order of $1–2\times10^7\,\mathrm{V\,cm^{-1}}$. An important aspect for the evolution of δ is the significant decrease in the energy difference between E_{ge} and $E_{ge'}/2$; at very large ground-state polarizations, all molecules approach a double resonance situation, which is most pronounced for molecule **VI** (vide supra). Thus, the energy-related term in the 3-state model (× in Figure 7) is strongly enhanced for large ground-state polarizations.

M_{ge} steadily increases with electric field in all molecules apart from **VI**, see Figure 8 (in the latter, this is caused by an increasing transition dipole to a second one-photon allowed state ($2B_u$) for large electric fields; however the impact of channels involving that state remains small).[37] Both the evolution of M_{ge} and the decreased detuning for large ground-state polarizations should consequently result in TPA cross sections increasing strongly with polarization. However, these effects are more than compensated by the evolution of the coupling between the one- and two-photon states; after slightly increasing for moderate fields, $M_{ee'}$ indeed collapses at large ground-state polarizations, see Figure 8.

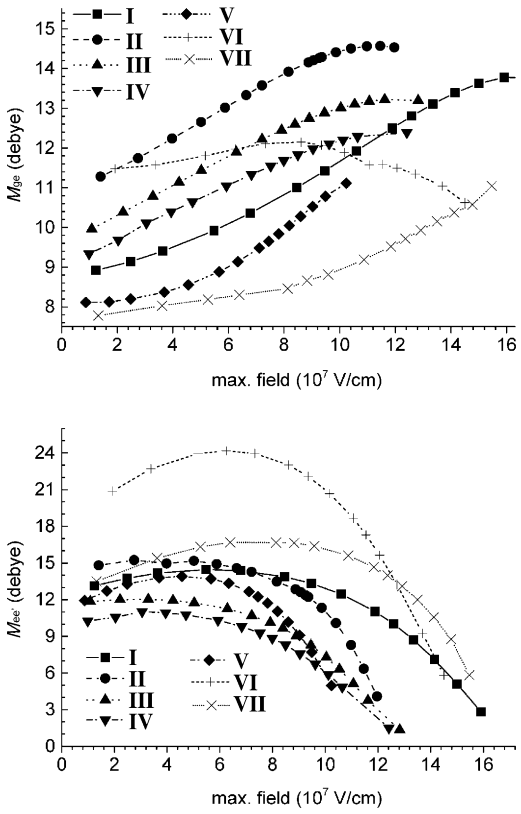

Figure 8. Evolution of the transition dipole moments between the ground state and the lowest one-photon allowed state (M_{ge}, top) and between the one-photon state and the lowest strongly two-photon-allowed state ($M_{ee'}$, bottom) as a function of the maximum electric field along the molecular axis induced by the point charges.

We have shown earlier for donor/acceptor-substituted stilbenes (molecule **I** in the present study) that this collapse is a consequence of a redistribution of oscillator strength as a result of electron-correlation effects.[15] The evolution of $M_{ee'}$ calculated in all molecules investigated here can be traced back to a similar origin: the observed weakening of the transition dipoles between the $1B_u$ and $2A_g/3A_g$ states at large ground-state polarizations is accompanied by an increase of the transition dipoles to a higher lying state, which is identified as the mA_g state discussed above. Thus, TPA cross sections well in excess of the already high values reported in Table 2 could be expected. However, the evolution of the mA_g energies with increasing ground-state polarization is nearly parallel to that of the $2A_g/3A_g$ energies. Since in our calculations, the mA_g energies at zero field are significantly higher than those of $2A_g/3A_g$ (see Table 2), at ground-state polarizations for which $M_{ee''}$ has strongly benefited from oscillator strength redistribution, the mA_g states lie at more than twice the energies of the $1B_u$ states. In such a case, they cannot be exploited for TPA applications.

In the CI approach, the correlation effects responsible for the redistribution of oscillator strength are expressed by a mixing of excited configurations. As mentioned above, there is a significant difference between group 1 and group 2 molecules. In the group 1 molecules (**I**, **V**, **VI**, and **VII**), the CI description of the $2A_g$ state for small ground-state polarizations is largely dominated by the $|\mathrm{H}-1\rightarrow\mathrm{L}\rangle$ excited determinant (one-electron excitation from the HOMO−1 to the LUMO), while for larger ground-state polarizations, the doubly excited $|\mathrm{H,H}\rightarrow\mathrm{L,L}\rangle$ determinant (both electrons promoted from the HOMO to the LUMO) plays an increasing role. As a first approximation, namely neglecting all other determinants contributing to the description of $2A_g$ and mA_g, the transition dipole moments $M_{ee'}$ and $M_{ee''}$ can be written as Equations (5a) and (5b):

$$M_{ee'} = C_{|\mathrm{H}-1\rightarrow\mathrm{L}\rangle,e'}\langle 1B_u|\hat{\mu}|\mathrm{H}-1\rightarrow\mathrm{L}\rangle + C_{|\mathrm{H,H}\rightarrow\mathrm{L,L}\rangle,e'}\langle 1B_u|\hat{\mu}|\mathrm{H,H}\rightarrow\mathrm{L,L}\rangle \quad (5a)$$

$$M_{ee''} = C_{|\mathrm{H}-1\rightarrow\mathrm{L}\rangle,e''}\langle 1B_u|\hat{\mu}|\mathrm{H}-1\rightarrow\mathrm{L}\rangle + C_{|\mathrm{H,H}\rightarrow\mathrm{L,L}\rangle,e''}\langle 1B_u|\hat{\mu}|\mathrm{H,H}\rightarrow\mathrm{L,L}\rangle \quad (5b)$$

in which the C's denote the CI coefficients of the relevant determinants in the description of the $2A_g$ and mA_g wavefunctions and $\hat{\mu}$ is the transition dipole operator. For the $2A_g$ states, Equation (5a), the transition dipole moments between $1B_u$ and these two determinants point in different directions (and therefore partly cancel each other); in contrast, they add in the case of the mA_g states, Equation (5b).[38] This does not play a significant role for small ground-state polarizations, since $C_{|\mathrm{HH}\rightarrow\mathrm{LL}\rangle,e'}$ is then relatively small, as shown in the top graph of Figure 9 for molecules **I** and **VII**. However, for large ground-state polarizations, the mixing of the two determinants increases, namely, the absolute values of the CI coefficients in Equations (5a) and (5b) approach each other (see Figure 9). Taking Equations (5a) and (5b) and the partial cancellation or addition of the two transition dipoles into account, this increased mixing (increased electron correlation) is responsible for the collapse of $M_{ee'}$ and the concomitant increase of $M_{ee''}$.

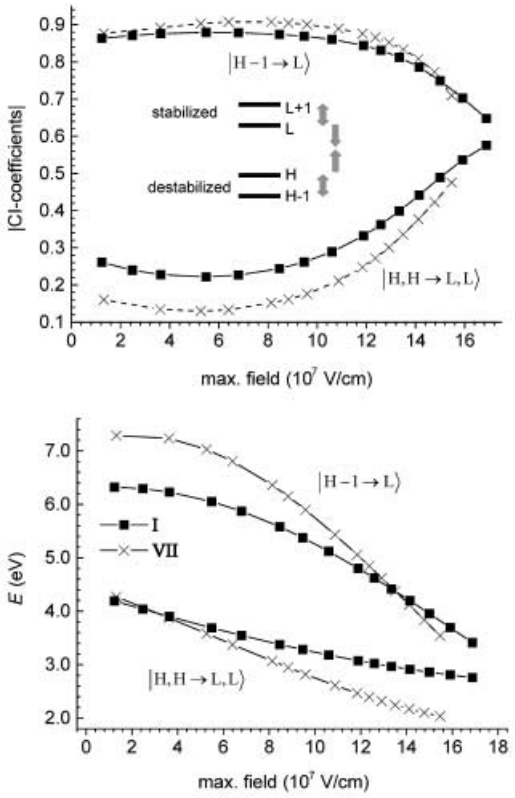

Figure 9. Top: Evolution of the CI coefficients of the $|H-1\rightarrow L\rangle$ and $|H,H\rightarrow L,L\rangle$ determinants in the description of the $2A_g$ states of molecules **I** (■) and **VII** (×); the inset provides a schematic representation of the evolution of the molecular orbital energies. Bottom: Energies of the $|H-1\rightarrow L\rangle$ and $|H,H\rightarrow L,L\rangle$ determinants as a function of the maximum electric field along the molecular axis induced by the point charges.

This explanation applies to all group 1 molecules. The origin of this effect can be qualitatively understood from the evolution of the molecular orbital energies: the donor and acceptor substitutions and the additional electric fields tend to destabilize the occupied frontier orbitals and to stabilize the unoccupied ones. This results in a strong decrease of the HOMO–LUMO gap with increasing ground-state polarization. The gap between HOMO−1 and HOMO, however, slightly increases in all molecules studied here, since the HOMO−1 is not as strongly destabilized by the substituents as the HOMO. Therefore, on the basis of the molecular orbital energies, the energy difference between the $|H-1\rightarrow L\rangle$ and $|H,H\rightarrow L,L\rangle$ determinants is expected to decrease with increasing ground-state polarization. This holds true also when considering the actual energies of the excited determinants (including the Coulomb and exchange contributions to the excitation energies), as shown in the bottom part of Figure 9. The decreased energy splitting between determinants in turn results in an increased mixing and thus in the transition dipole redistribution discussed above.[39]

Also for the group 2 molecules, a strong excited determinant mixing occurs for large ground-state polarizations. The collapse of the $M_{ee'}$ transition dipole can thus also be associated with correlation effects. An explanation on the basis of orbital energies is, however, more complex; indeed in group 2 molecules, the doubly excited $|H,H\rightarrow L,L\rangle$ determinant enters primarily into the description of the $2A_g$ state, which displays weak TPA (see above), while the evolution of $3A_g$ is dominated by the mixing of $|H-1\rightarrow L\rangle$ with $|H\rightarrow L+1\rangle$ (and, at large ground-state polarizations, also with other doubly excited determinants).

Another interesting effect is that, while $\overrightarrow{M}_{ge}$ and $\overrightarrow{M}_{ee'}$ are virtually parallel at small ground-state polarizations, the angle between them significantly increases for the largest electric fields considered in our studies: in **I**, the angle increases from 7° to 31°; in **II**, from 0° to 21°; in **III**, from 1° to 46°; in **IV**, from 19° to 44°; in **V** from 12° to 32°; and in **VI**, from 7° to 40° for the field range for which $M_{ee'}$ is reported in Figure 8. This is attributed to a decrease in the $\overrightarrow{M}_{ee'}$ component parallel to the long molecular axis and an increase in the component perpendicular to it. This can be understood from the corresponding transition densities shown in Figure 10 for various electric fields (covering the field range for which values are given in Figure 8). Here, molecules **II** and **VI** are chosen as representative examples for group 1 and group 2 systems, respectively. At small ground-state polarizations, $\overrightarrow{M}_{ee'}$ is dominated by transition densities along the molecular backbone (largely localized on the nitrogen atoms of the dimethylamino groups), while there is hardly any transition density on the cyano groups. At large ground-state polarizations (i.e., large external electric fields), the transition densities on the dimethylamino groups are strongly suppressed, leading to a major decrease

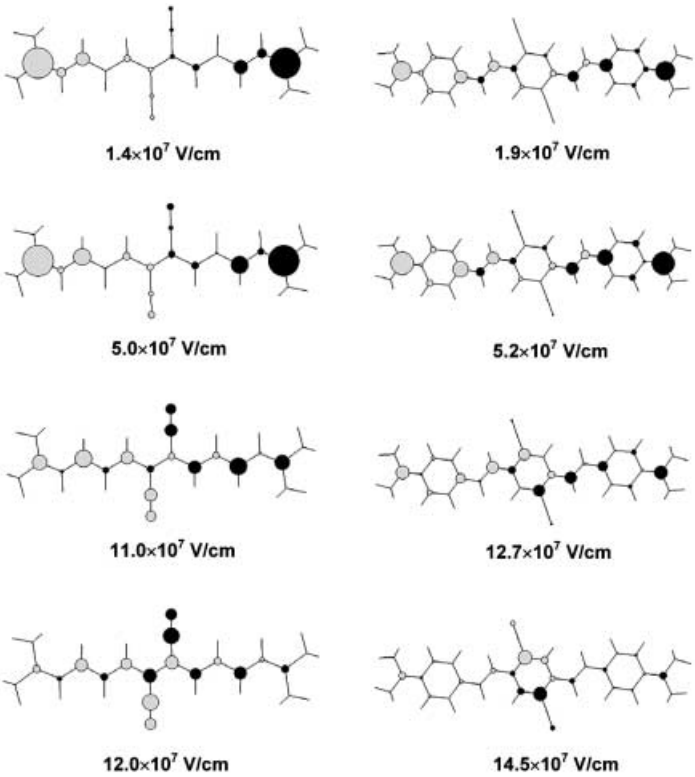

Figure 10. Transition densities associated with the $M_{ee'}$ transition dipole moment for fields ranging from the lowest applied field (point charges at a distance of 10 Å from the molecular plane) to the highest field for which $M_{ee'}$ is reported in Figure 8.

in the longitudinal transition dipole. The remaining transition densities are concentrated on the cyano groups (in **II**) and on the central phenylene ring (in **VI**). For those transition densities, the distances from the center of inversion of the molecules are small, which results in small contributions to the transition dipoles [Eq. (4)]; moreover, the resulting large angle between $\overrightarrow{M}_{ge}$ and $\overrightarrow{M}_{ee'}$ further reduces the effective value of $M_{ee'}$ according to Equation (6), as described in the Computational Methods section.

$$M_{ee'} = |\overrightarrow{M}_{ee'}|\sqrt{\cos^2\Theta + \frac{1}{3}\sin^2\Theta} \quad (6)$$

Conclusion

We have applied correlated quantum-chemical calculations to analyze the two-photon absorption response in a series of π-conjugated molecules, which are substituted by donor (D) and acceptor (A) groups in a D-A-D quadrupolar fashion. We have considered various backbones: stilbene, distirylbenzene, polyene, thienylenevinylene, and indenofluorene.

The molecules can be classified into two groups, depending on whether or not they have a one-photon forbidden $2A_g$ state below the $1B_u$ state. When this is the case (group 2 molecules), the TPA cross section into the $2A_g$ state is very small, but is significant into $3A_g$. For group 1 molecules, the dominant TPA active state in the low-energy region is $2A_g$. In both groups of molecules, we find a second TPA-active state at higher energies (mA_g), whose TPA cross section is strongly enhanced on account of a low energy-detuning factor. It was found that increasing the distance between the donor groups by increasing the conjugation length resulted in markedly higher δ values, while increasing the distance between the acceptors and the backbone (in a direction perpendicular to the long molecular axis) is rather detrimental to the TPA response. The largest δ value into the lowest TPA state is obtained for the polyene backbone ($\delta =$ 1500 GM), while the TPA cross sections for excitation into mA_g is about one order of magnitude higher.

To simulate the influence of stronger donor and acceptor groups and/or highly polar media, we have systematically increased the degree of ground-state polarization of the molecules by applying an external electric field in the form of quadrupolar point charge distributions. Interestingly, we find the same trends for all molecules: the TPA cross section first increases significantly (reaching values beyond 20000 GM for the polyene-type backbone) and then collapses for very large ground-state polarizations. The latter effect can be explained by an electron correlation-induced oscillator-strength redistribution.

Computational Methods

Optimizing the geometry: The molecular geometries were optimized with the semiempirical Austin Model1 (AM1) method.[40] When approaching the point charges toward the molecular plane, the bond lengths were reoptimized for each step. Note that we kept the bond angles at the values optimized for the molecules without point charges, in order to avoid artifacts related to distortions resulting from the electrostatic interactions among the point charges. These would lead to unreliable results, especially in the case of molecule **V**, for which a full optimization results in significantly curved bonds between the central vinylene units and the cyano groups. Test calculations with fully reoptimized geometries in compound **I**, one of the chromophores in which these effects play only a minor role, yielded no significant deviations from calculations in which the bond angles were kept fixed.

Excitation energies and transition dipoles: The electronic structure in the ground and excited states was calculated with the semiempirical Intermediate Neglect of Differential Overlap (INDO) Hamiltonian.[41] To account for correlation effects, which are essential to describe properly TPA-active states,[33,15] the INDO Hamiltonian was coupled to a Multi-Reference-Determinant Single-and-Double-Configuration-Interaction technique (MRD-CI).[42,43] This technique has been found to provide excitation energies and dipole matrix elements in good agreement with experiment.[5,44] The Mataga–Nishimoto (MN) potential[45] was used to describe the Coulomb repulsion terms, as it is our experience that this potential usually yields a better agreement with a number of spectroscopic data[12,46,47] than the Ohno–Klopman (OK) potential[48] used in several previous studies[5,8,19] (to insure that the overall effects described in this work are parameter independent, we also performed extensive tests with the Ohno–Klopman potential; although the exact values of transition energies and transition matrix elements somewhat differ between the two potentials, the trends are very similar; a more extended comparison can be found in ref. [15]).

The CI-active space was scaled according to the size of the molecules (apart from molecule **VI**, where for higher excitations we were limited to the same active orbitals as in **I**). We included the single excitations between all π-orbitals and the perpendicular π orbitals in the CN groups. For higher excited determinants, the CI-active space had to be restricted owing to size limitations (**I**, **VI**, **VII**: six highest occupied to six lowest unoccupied π orbitals; **II**: five highest occupied to five lowest unoccupied π orbitals; **III** and **IV**: six highest occupied to five lowest unoccupied π orbitals; **V**: between six occupied and six unoccupied π orbitals that are equivalent to the orbitals chosen for the description of **I**). Care was taken to ensure that equivalent orbitals were selected for the various molecules; for increasing ground-state polarizations (when the order of the orbitals changes), we used the orbitals at low ground-state polarization as prototypes for the selection of the CI active space. The reference determinants included in all molecules were the SCF determinant as well as the determinants in which one or two electrons are promoted from the HOMO to the LUMO. Additional reference determinants were considered when they strongly contributed to the description of the studied one- and two-photon allowed states (these were the HOMO−1→LUMO determinant in all molecules, the HOMO→LUMO+1 determinant in **II**, **III**, **IV** and **VII**, and the HOMO−1→LUMO+1 determinant in **VII**).

Calculating the TPA cross section: The calculation of the TPA cross section from the TPA tensor was discussed above in the section on the theoretical approach. It has been shown[49] that this method is equivalent to calculating δ from the frequency-dependent imaginary part of the third-order polarizability γ, when using the perturbative Sum-Over-States (SOS) expression given by Orr and Ward[50] and retaining only those terms that contain a two-photon resonance to a given state $|e'\rangle$. The latter method has been applied in numerous previous studies. We found deviations between the two methods only when approaching a double-resonance situation in which the energy of the two-photon state was nearly twice that of the one-photon state. These differences are discussed below.

When calculating the TPA cross section from the two-photon tensor S, for the sake of consistency, we chose Lorenzian's lineshape functions with a full width at half maximum set to twice the value of the damping factor Γ in the SOS expression.[51] To ease comparison with previous studies, we then reported the maximum values of the resulting peaks in δ for excitation to a particular state $|e'\rangle$. Γ was set to 0.1 eV, in agreement with previous investigations. (Possible differences in the homogeneous and inhomogeneous broadening in different materials were not considered. Choosing a correspondingly modified width for the normalized lineshape functions would influence the values of the TPA maxima, but not the TPA response integrated over the full spectral feature.)

Note that, in general, the transition dipoles among the various excited states were not fully parallel. For calculations that employ the full expression for $S_{e'}$ (denoted as δ_{TEN}), this aspect was accounted for by the tensor nature of $S_{e'}$ and the averaging according to Equation (2). However, when the converged results are analyzed with the three-state model given in Equation (3), $M_{ee'}$ had to be viewed as an effective transition dipole. In the investigated molecules, the angle between $\overrightarrow{M}_{ge}$ and $\overrightarrow{M}_{ee'}$ was usually very small, but it can reach values of up to 40° for large ground-state polarizations. According to Cronstrand et al.,[10] the effective transition dipole describing $\overrightarrow{M}_{ee'}$ in the 3-state model is determined by the norm of the transition dipole vector $|\overrightarrow{M}_{ee'}|$ and Θ, the angle between the transition dipole vectors $\overrightarrow{M}_{ge'}$ and $\overrightarrow{M}_{ee'}$ [Eq. (6)]. Thus, whenever analyzing trends based on the 3-state model, the values of $M_{ee'}$ are given instead of $|\overrightarrow{M}_{ee'}|$.

Deviations between δ values calculated from the TPA tensor (δ_{TEN}) and from Im(γ) using the SOS approach (δ_{SOS}): When calculating δ from Im(γ) with the SOS algorithm (δ_{SOS}), significant deviations from δ_{TEN} were found only when approaching a double-resonance situation, namely, when the photon energy for nonlinear absorption approached that for linear absorption. This is related to the fact that Im(γ) and consequently δ_{SOS} not only contain two-photon absorption contributions, but are proportional to the overall nonlinear absorption cross section that can contain contributions from other processes, such as ground-state bleaching. This can be shown, for example, by solving the damped nonlinear wave equations. When approaching the region of linear absorption, effects, such as ground-state bleaching, start to play a role. In fact, terms similar to the microscopic description of ground-state bleaching can be identified in the negative resonances in the SOS description of Im(γ) around the one-photon absorption energy. As these effects are intensity-dependent and reduce the overall absorption coefficient in the spectral region around the one-photon resonance, they give a negative contribution to the nonlinear absorption coefficient. This can be seen, for example, in Figure 11 for the evolution of δ_{SOS}. The general trends are similar to those shown in Figure 5 for δ_{TEN}; however, as the ground-state polarization is increased, δ_{SOS} collapses at much smaller applied fields than δ_{TEN}. This is because the δ values plotted in Figure 11 are the maxima of the energy-dependent nonlinear absorption cross section including all excited states and thus are determined by the overlap of the true TPA features with the negative resonances originating from ground-state bleaching. These effects also affect the TPA cross sections to the higher lying A_g states in compounds **III** and **IV** (see Table 2).

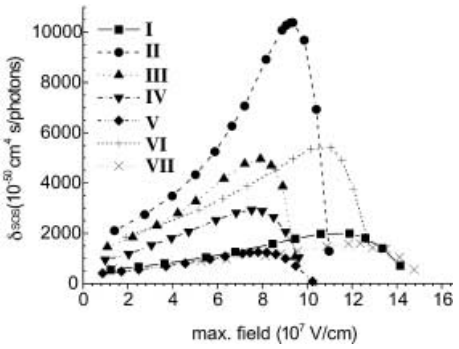

Figure 11. INDO/MRDCI calculated evolution of the converged TPA cross section as a function of the strength of the donor and acceptor groups expressed as the maximum electric field along the long molecular axes induced by the point charges. δ_{SOS} is derived from the full sum-over-states expression for Im(γ). The δ values for the peaks in the calculated TPA spectra are given in this graph.

At this point, one should note that the perturbative description applied in the SOS approach (which assumes, for instance, an identical damping for all excited states) cannot provide a proper description of ground-state bleaching effects. One of the reasons is that the lifetimes, which correspond to the damping factors in the SOS expression, are related to the dephasing times of the system, while ground-state bleaching is determined by the total incoherent lifetime of the S_1 state. Therefore, the description of TPA by δ_{SOS} at energies relatively close to one-photon absorption features has to be considered with care.

Acknowledgement

The authors would like to thank G. Jakopic and Z. Shuai for fruitful discussions. The work at Arizona is partly supported by the Air Force Office of Scientific Research, the University of Arizona Photonics Initiative, the NSF (through the STC for Materials and Devices for Information Technology Research DMR-0120967), and the IBM Shared University Research Program. Financial support by the Austrian Spezialforschungsbereich Elektroaktive Stoffe is acknowledged. The work in Mons is carried out within the framework of the Belgium Prime Minister Office of Science Policy program "Pôle d'Attraction Interuniversitaire en Chimie Supramoléculaire et Catalyse (PAI 5/3)" and is partly supported by the Belgium National Fund for Scientific Research (FNRS-FRFC). DB is an FNRS Senior Research Associate.

[1] A. A. Said, C. Wamsley, D. J. Hagan, E. W. van Stryland, B. A. Reinhardt, P. Roderer, A. G. Dillard, *Chem. Phys. Lett.* **1994**, *228*, 646; J. D. Bhawalkar, G. S. He, P. N. Prasad, *Rep. Prog. Phys.* **1996**, *59*, 1041; J. E. Ehrlich, X. L. Wu, Ys. L. Lee, Z. Y. Hu, H. Rockel, S. R. Marder, J. W. Perry, *Opt. Lett.* **1997**, *22*, 1843.

[2] D. A. Parthenopoulos, P. M. Rentzepis, *Science* **1989**, *245*, 843; J. H. Strickler, W. W. Webb, *Opt. Lett.* **1991**, **16**, 1780; B. H. Cumpston, S. P. Ananthavel, S. Barlow, D. L. Dyer, J. E. Ehrlich, L. L. Erskine, A. A. Heikal, S. M. Kuebler, I.-Y. S. Lee, D. McCord-Maughon, J. Qin, H. Röckel, M. Rumi, X.-L. Wu, S. R. Marder, J. W. Perry, *Nature* **1999**, *398*, 51; W. H. Zhou, S. M. Kuebler, K. L. Braun, T. Y. Yu, J. K. Cammack, C. K. Ober, J. W. Perry, S. R. Marder, *Science* **2002**, *296*, 1106; S. Kawata, H.-B. Sun, T. Tanaka, K. Takada, *Nature* **2001**, *412*, 697.

[3] W. Denk, J. H. Strickler, W. W. Webb, *Science* **1990**, *248*, 73–76; R. H. Köhler, J. Cao, W. R. Zipfel, W. W. Webb, M. R. Hanson, *Science* **1997**, *276*, 2039; M. J. Miller, S. H. Wei, I. Parker, M. D. Cahalan, *Science* **2002**, *296*, 1869.

[4] D. L. Pettit, S. S. H. Wang, K. R. Gee, G. J. Augustine, *Neuron* **1997**, *19*, 465.

[5] M. Albota, D. Beljonne, J.-L. Brédas, J. E. Ehrlich, J.-Y. Fu, A. A. Heikal, S. E. Hess, T. Kogej, M. D. Levin, S. R. Marder, D. McCord-Maughon, J. W. Perry, H. Röckel, M. Rumi, G. Subramaniam, W. W. Webb, X.-L. Wu. Ch. Xu, *Science* **1998**, *281*, 1653.

[6] B. Reinhardt, L. L. Brott, S. J. Clarson, A. G. Dillard, J. C. Bhatt, R. Kannan, L. Yuan, G. S. He, P. N. Prasad, *Chem. Mater.* **1998**, *10*, 1863; R. Kannan, G. S. He, L. Yuan, F. Xu, P. N. Prasad, A. Dombroskie, B. A. Reinhardt, J. W. Baur, R. A. Vaia, L.-S. Tan, *Chem. Mater.* **2001**, *13*, 1896; C.-K. Wang, P. Macak, Y. Luo, H. Ågren, *J. Chem. Phys.* **2001**, *114*, 9813; L. Ventelon, S. Charier, L. Moreaux, J. Mertz, M. Blanchard-Desce, *Angew. Chem.* **2001**, *113*, 2156; *Angew. Chem. Int. Ed.* **2001**, *40*, 2098; A. Abotto, L. Beverina, R. Nozio, A. Facchetti, C. Ferrante, G. A. Pagani, D. Pedron, R. Signorini, *Org. Lett.* **2002**, *4*, 1495; B. Strehmel, A. M. Sarker, H. Detert, *ChemPhysChem* **2003**, *4*, 249.

[7] J. D. Bhawalkar, G. S. He, C.-K. Park, C. F. Zhao, G. Ruland, P. N. Prasad, *Opt. Commun.* **1996**, *124*, 33; G. S. He, L. Yuan, N. Cheng, J. D. Bhawalkar, P. N. Prasad, L. L. Brott, S. J. Clarson, B. A. Reinhardt, *J. Opt. Soc. Am. B* **1997**, *14*, 1079; G. S. He, L. Yuan, P. N. Prasad, A. Abotto, A. Facchetti, G. A. Pagani, *Opt. Commun.* **1997**, *140*, 49; A. Abotto, L. Beverina, R. Bozio, S. Bradamante, C. Ferrante, G. A. Pagani, R. Signorini, *Adv. Mater.* **2000**, *12*, 1963; A. Painelli, L. Del Freo, F. Terenziani, *Chem. Phys. Lett.* **2001**, *346*, 470; R. Zaleśny, W. Bartowiak, S. Styrcz, J. Leszczynski, *J. Phys. Chem. A* **2002**, *106*, 4032; H. Lei, Z. L. Huang, H. Z. Wang, X. J. Tang, L. Z. Wu, G. Y. Zhou, D. Wang, Y. B. Tian, *Chem. Phys. Lett.* **2002**, *352*, 240.

[8] T. Kogej, D. Beljonne, F. Meyers, J. W. Perry, S. R. Marder, J.-L. Brédas, *Chem. Phys. Lett.* **1998**, *298*, 1.

[9] M. Rumi, J. E. Ehrlich, A. A. Heikal, J. W. Perry, S. Barlow, Z. Hu, D. McCord-Maughon, T. C. Parker, H. Röckel, S. Thayumanavan, S. R. Marder, D. Beljonne, J.-L. Brédas, *J. Am. Chem. Soc.* **2000**, *122*, 9500; M. Barzoukas, M. Blanchard-Desce, *J. Chem. Phys.* **2000**, *113*, 3951; O. Mongin, L. Porrès, L. Moreaux, J. Mertz, M. Blanchard-Desce, *Org. Lett.* **2002**, *4*, 719.

[10] P. Cronstrand, Y. Luo, H. Ågren, *Chem. Phys. Lett.* **2002**, *352*, 262.

[11] S.-J. Chung, K.-S. Kim, T.-Ch. Lin, G. S. He, J. Swiatkiewicz, P. N. Prasad, *J. Phys. Chem. B* **1999**, *103*, 10741; W.-H. Lee, H. Lee, J.-A Kim, J.-H. Choi, M. Cho, S.-J. Jeon, B. R. Cho, *J. Am. Chem. Soc.* **2001**, *123*, 10658; B. R. Cho, M. J. Piao, K. H. Son, S. H. Lee, S. J. Yoon, S.-J. Jeon, M. Cho, *Chem. Eur. J.* **2002**, *8*, 3907.

[12] D. Beljonne, E. Zojer, Z. Shuai, H. Vogel, W. Wenseleers, S. J. K. Pond, J. W. Perry, S. R. Marder, J.-L. Brédas, *Adv. Funct. Mater.* **2002**, *12*, 631.

[13] A. Adronov, J. M. J. Fréchet, G. S. He, K. S. Kim, S. J. Chung, J. Swiatkiewicz, P. N. Prasad, *Chem. Mater.* **2000**, *12*, 2838; M. Drobizhev, A. Karotki, A. Rebane, C. W. Spangler, *Opt. Lett.* **2001**, *26*, 1081; O. Mongin, J. Brunel, L. Porrès, M. Blanchard-Desce, *Tetrahedron Lett.* **2003**, *44*, 2813.

[14] M. Drobizhev, A. Karotki, M. Mruk, N. Zh. Mamardashvili, A. Rebane, *Chem. Phys. Lett.* **2002**, *361*, 504.

[15] E. Zojer, D. Beljonne, T. Kogej, H. Vogel, S. R. Marder, J. W. Perry, J.-L. Brédas, *J. Chem. Phys.* **2002**, *116*, 3646.

[16] S. R. Marder, Ch. B. Gorman, F. Meyers, J. W. Perry, G. Bourhill, J.-L. Brédas, B. M. Pierce, *Science* **1994**, *265*, 632.

[17] F. Meyers, S. R. Marder, J. W. Perry, G. Bourhill, S. Gilmour, L. T. Cheng, B. M. Pierce, and J.-L. Brédas, *MCLC S&T Sect. B* **1995**, *9*, 59; S. R. Marder, W. E. Torruellas, M. Blanchard-Desce, V. Ricci, G. I. Stegeman, S. Gilmour, J.-L. Brédas, J. Li, U. Bublitz, S. G. Boxer, *Science* **1997**, *276*, 1233.

[18] J.-L. Brédas, C. Adant, P. Tackx, A. Persoons, B. M. Bierce, *Chem. Rev.* **1994**, *94*, 243; F. Meyers, S. R. Marder, B. M. Pierce, J.-L. Brédas, *J. Am. Chem. Soc.* **1994**, *116*, 10703.

[19] S. J. K. Pond, M. Rumi, M. D. Levin, T. C. Parker, D. Beljonne, M. W. Day, J.-L. Brédas, S. R. Marder, J. W. Perry, *J. Phys. Chem. A* **2002**, *106*, 11470.

[20] C. G. Gorman S. R. Marder, *Proc. Natl. Acad. Sci. USA* **1993**, *90*, 11297.

[21] S. R. Marder, J. W. Perry, G. Bourhill, Ch. B. Gorman, B. G. Tiemann, K. Mansour, *Science* **1993**, *261*, 186.

[22] P. R. Monson , W. M. McClain, *J. Chem. Phys.* **1970**, *53*, 29.

[23] W. L. Peticolas, *Annu. Rev. Phys. Chem.* **1967**, *18*, 233.

[24] We use δ here, as the value calculated with Equation (2) (before considering a lineshape function) corresponds to the integral TPA cross section into a particular excited state, while the values usually given in the literature correspond to peak values.

[25] S. Mazumdar, D. Duo, S. N. Dixit, *Synth. Met.* **1993**, *55*, 3881; S. Mazumdar, F. J. Guo, *J. Chem. Phys.* **1994**, *100*, 1554; C. W. Dirk, L. T. Cheng, M. G. Kuzyk, *Mater. Res. Soc. Symp. Proc.* **1992**, *247*, 80.

[26] Molecule **VII** is the only molecule in which δ_{approx} underestimates the converged value of δ. This is partly caused by a second one-photon allowed state that contributes to the TPA cross section into $2A_g$ by means of the interference term discussed in reference [10]. The contribution is, however, only minor compared to the primary excitation channel and diminishes for increasing ground-state polarization. Another reason for the increased δ_{TEN} compared to δ_{approx} in **VII** is a second TPA active state located only 0.6 eV above the $2A_g$ state.

[27] In **II**, **IV**, and **VII**, the differences between planarized and fully relaxed conformations is much smaller, as the only slight deviations from planarity are found in the dimethylamino substituents.

[28] The significantly smaller calculated transition matrix elements given in reference [19] are mainly a consequence of the use of the Ohno–Klopman potential in that publication.

[29] A reliable study of the conjugation-length dependence of TPA requires highly correlated size-consistent methods. A possible candidate is the semiempirical coupled-cluster/equation-of-motion approach, see: Z. Shuai, J.-L. Brédas, *Phys. Rev. B* **2000**, *62*, 15452.

[30] J. R. Heflin, K. Y. Wong, O. Zamani-Khamiri, A. F. Garito, *Phys. Rev. B* **1988**, *38*, 1573.

[31] Z. G. Soos, D. S. Galvão, S. Etemad, *Adv. Mater.* **1994**, *6*, 280, and references therein.

[32] F. Guo, D. Guo, S. Mazumdar, *Phys. Rev. B* **1994**, *49*, 10102.

[33] P. Tavan, K. Schulten, *J. Chem. Phys.* **1986**, *85*, 6602; P. Tavan, K. Schulten, *Phys. Rev. B* **1987**, 36, 4337; B. M. Pierce, *J. Chem. Phys.* **1989**, *91*, 791; Z. Shuai, D. Beljonne, J.-L. Brédas, *J. Chem. Phys.* **1992**, *97*, 1132; D. Guo, S. Mazumdar, S. N. Dixit, F. Kajzar, F. Jarka, Y. Kawabe, N. Peyghambarian, *Phys. Rev. B* **1993**, *48*, 1433.

[34] Z. G. Soos, D. S. Galvão, *J. Phys. Chem.* **1994**, *98*, 1029.

[35] S. K. Pati, T. J. Marks, M. A. Ratner, *J. Am. Chem. Soc.* **2001**, *123*, 7287.

[36] Defined as the maximum field strength along the axis connecting the two nitrogen atoms of the donors.

[37] The transition dipole between the $2B_u$ and the $2A_g$ (lowest TPA state) states ranges from 1 D for small to 5 D for large ground-state polarizations; one might therefore expect the channels involving $2B_u$ to play a significant role in the SOS expression for very large ground-state polarizations, as then the coupling between the $1B_u$ and $2A_g$ states decreases (see Figure 8). However, in that case, the detuning with respect to the $1B_u$ state vanishes, while it is still large with respect to $2B_u$, even at large ground-state polarizations. Therefore, the contributions arising from channels through $2B_u$ (including the interference terms described in ref. [10]) remain very small.

[38] At this point it should be noted that we observe a splitting of the mA_g states for certain ground-state polarizations, which can be explained by a strong interference with other excited determinants at these particular molecular structures.

[39] The eigenstates of the Hamiltonian (approximately corresponding to the $2A_g$ and mA_g states) in the space spanned by the two excited determinants are given by Equation (7) (in which 1 denotes

$$|\Psi\rangle_n = c_{1,n}|H-1\rightarrow L\rangle + c_{2,n}|H,H\rightarrow L,L\rangle$$
$$c_{2,n} = \frac{H_{22}-H_{11}\pm\sqrt{(H_{11}-H_{22})^2+4H_{12}^2}}{2H_{12}}c_{1,n} \qquad (7)$$

the $|H-1\rightarrow L\rangle$ and 2 denotes the $|H,H\rightarrow L,L\rangle$ determinants). As the energies of the two determinants approach each other ($H_{11}\rightarrow H_{22}$), they enter with equal weights into the description of $|\Psi\rangle_n$. The transition dipoles coupling the $1B_u$ state to the above eigenstates then are given by Equation (8).

$$M_{ee',H11\rightarrow H22} = \frac{1}{\sqrt{2}}\left(\langle 1B_u|\hat{\mu}|H-1\rightarrow L\rangle - \langle 1B_u|\hat{\mu}|H,H\rightarrow L,L\rangle\right)$$
$$M_{ee'',H11\rightarrow H22} = \frac{1}{\sqrt{2}}\left(\langle 1B_u|\hat{\mu}|H-1\rightarrow L\rangle + \langle 1B_u|\hat{\mu}|H,H\rightarrow L,L\rangle\right) \qquad (8)$$

[40] M. J. S. Dewar, E. G. Zoebisch, E. F. Healy, J. J. P. Stewart, *J. Am. Chem. Soc.* **1985**, *107*, 3902.

[41] J. A. Pople, D. L. Beveridge, P. A. Dobosh, *J. Chem. Phys.* **1967**, *47*, 2026; J. Ridley, M. Zerner, *Theor. Chim. Acta* **1973**, *32*, 111.

[42] R. J. Buenker, S. D. Peyerimhoff, *Theor. Chim. Acta* **1974**, *35*, 33.

[43] K. Schulten, M. Karplus, *Chem. Eng. Sci. Chem. Phys. Lett.* **1972**, *14*, 305.

[44] See, for example: P. Tavan, K. Schulten *Phys. Rev. B* **1987**, *36*, 4337; Z. Shuai, D. Beljonne, J.-L. Brédas, *J. Chem. Phys.* **1992**, *97*, 1132; D. Beljonne, J.-L. Brédas, *Phys. Rev. B* **1994**, *50*, 2841; D. Beljonne, Z. Shuai, R. H. Friend, J.-L. Brédas, *J. Chem. Phys.* **1995**, *102*, 2042; D. Beljonne, G. E. O'Keefe, P. J. Hamer, R. H. Friend, H. L. Anderson, J.-L. Brédas, *J. Chem. Phys.* **1997**, *106*, 9439.

[45] N. Mataga, K. Nishimoto, *Z. Phys. Chem.* **1957**, *13*, 140.

[46] M. Halik, W. Wenseleers, C. Grasso, F. Stellacci, E. Zojer, S. Barlow, J.-L. Brédas, J. W. Perry, S. R. Marder, *Chem. Commun.* **2003**, 1490; E. Zojer, W. Wenseleers, M. Halik, C. Grasso, S. Barlow, J. W. Perry, Seth R. Marder, J.-L. Brédas, *ChemPhysChem* in press.

[47] This observation is probably related to the stronger screening included in the Mataga–Nishimoto potential, which could be more appropriate to describe experiments performed in solution.
[48] K. Ohno, *Theor. Chim. Acta* **1964**, *2*, 219; G. Klopman, *J. Am. Chem. Soc.* **1964**, *86*, 4550.
[49] Y. Luo, P. Norman, P. Macak, H. Ågren, *J. Phys. Chem. A* **2000**, *104*, 4718.
[50] B. J. Orr, J. F. Ward, *Mol. Phys.* **1971**, *20*, 513.
[51] Owing to the description of damping in Ref. [50], this yields the same linewidths for both approaches.

Received: October 21, 2003
Published online: April 15, 2004

